

# Image Pre-Compensation to Facilitate Computer Access for Users with Refractive Errors

Miguel Alonso Jr.

Digital Signal Processing Laboratory  
Florida International University  
Miami, FL 33174 USA  
+1 305 348 6072

miguel.alonso@fiu.edu

Armando Barreto

Electrical and Computer Engineering  
Department  
Florida International University  
Miami, FL 33174 USA  
+1 305 348 3711

barretoa@fiu.edu

J. Gualberto Cremades

School of Human Performance and  
Leisure Science  
Barry University  
Miami Shores, FL 33161 USA  
+1 305 899 4846

gcremades@mail.barry.edu

## ABSTRACT

The use of computer technology for everyday tasks has become increasingly important in today's world. Frequently, computer technology makes use of Graphical User Interfaces (GUIs), presented through monitors or LCD displays. This type of visual interface is not well suited for users with visual limitations due to refractive errors, particularly when they are severe and not correctable by common means.

In order to facilitate computer access for users with refractive deficiencies, an algorithm was developed, using a priori knowledge of the visual aberration, to generate an inverse transformation of the images that are then displayed on-screen, countering the effect of the aberration. The result is that when the user observes the screen displaying the transformed images, the image perceived in the retina will be similar to the original image.

The algorithm was tested by artificially introducing a spherical aberration in the field of view of 14 subjects, totaling 28 individual eyes. Results show that when viewing the screen, this method of compensation improves the visual performance of the subjects tested in comparison to viewing uncompensated images.

## Categories and Subject Descriptors

I.4.9 [Image Processing and Computer Vision]: Applications

## General Terms

Algorithms, Measurement, Performance, Design, Experimentation, Human Factors, Theory.

## Keywords

Low Vision, Visual Aberration, Wavefront Aberration, Point Spread Function, Compensation, Deconvolution, Deblurring.

## 1. INTRODUCTION

In interacting with computers, human beings rely heavily on their sense of vision. Thus, if there are any aberrations present in the

user's visual system, their effective use of the personal computer is hindered. This, in turn, restricts those users in many of their everyday activities.

Optical lenses have been used to overcome visual limitations, such as defocus, in one way or another since the XIII Century. Developments in ophthalmology during the last century have arisen to compensate for these aberrations in the form of contact lenses, and recently, LASIK surgery. These forms of correction however, can only deal with what are known as low-order aberrations. They are ill-suited to deal with high-order aberrations, characteristic, for example, of a corneal degeneration known as keratoconus [14].

There have been attempts to compensate for the visual aberrations in the human eye [8, 13, 17]. These methods however, are bulky and require very expensive custom equipment. Thibos [17] proposes the use of a spatial light modulator to provide the compensation, much the same way glasses do. Jiang et al. [13] provide the compensation via a deformable mirror and an online method of measuring the aberration of the user. Although these methods are effective, their complexity and high cost render them impractical for everyday use.

In contrast with the optical correction of visual limitations, the approach described here is based on modifying the image at its source, i.e., applying image processing modifications on the image to be displayed on-screen before it is shown to the user, based on the knowledge of his/her own wavefront aberration function. Additionally, this method should apply equally well to both low-order (myopia, hyperopia, etc.) as well as high order aberrations (keratoconus). The aim of the pre-compensation proposed is to modify the intended display image in a way that is opposite to the effect of the wavefront aberration of the eye. Once this is achieved, the result is displayed to the viewer so that the wavefront aberration in the viewer's eye will "cancel" the pre-compensation, resulting in the projection of an undistorted version of the intended image on the retina. The method outlined here could leverage the power of personal computers (PCs) already available to the intended users.

With knowledge of the user's visual aberration, it is possible to generate images to be displayed on-screen that pre-compensate for the aberration present in the user's eye, without requiring additional equipment.

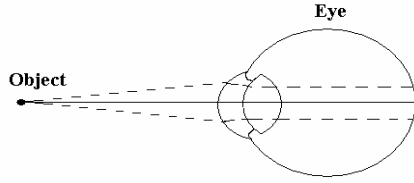


**Figure 1. Spreading of a point object due to visual impairment**

The paper is organized as follows. We begin by introducing the problem with examples presenting the degradation in image quality when aberrations are present. The approach proposed to compensate for these aberrations is then outlined, following with a description of the procedure used in the evaluation of the proposed approach, the results, and the conclusions drawn.

## 2. PROBLEM STATEMENT

Our visual perspective of the world is formed by the projection of the image of the objects in that world against the retina, the light sensitive portion of the human eye. The retina is composed of rods and cones, which generate action potentials when stimulated by light [7]. The human eye, being an imaging system, behaves in a manner similar to any type of imaging system composed of lenses [16], which form an image at their effective focal length.

Any object, when being viewed by the eye, can be thought of as a two-dimensional array of points, each varying with intensity [19]. Thus, for an aberration-free eye, each point in the object is represented as a point on the retina, at the focal length of the eye's lens. In the context of human-computer interface, when the user views the computer screen, each pixel can be thought of as a point-source of light, and the corresponding image of that pixel is projected onto the retina.

If the eye is unable to project a point source of light onto the retina as a corresponding point, the result is a broad Point Spread Function (PSF), causing the point source of light to be projected not at one point, but rather at multiple points on the retina, which introduces a blurring effect in the retinal image (Figure 1).

The PSF of the human eye can be found indirectly through what is known as the wavefront aberration function, which represents the deviation of the light wavefront from a purely spherical pattern as it passes the pupil on its way to the retina [15]. In an unaberrated eye, the refracted light is organized in the form of a uniform spherical wavefront, converging to the paraxial focal point on the retina.

Modern day solutions can only offer limited corrections for those individuals whose visual impairments are not severe. But for some individuals whose visual impairments are very severe, a more robust system of visual compensation is necessary.

### 2.1 The Human Eye as a Linear Time Invariant System

For many applications, optical systems can be thought of as Linear Time Invariant (LTI) systems [6]. Within this framework, all of the rules that apply to conventional LTI systems also apply to the optical system.

Let us consider that the retinal image,  $U'(x,y)$  is formed by the convolution of the system input,  $U(x,y)$ , with the system's two-dimensional impulse response, or PSF,  $H(x,y)$ :

$$U'(x, y) = U(x, y) \otimes H(x, y) \quad (1)$$

where  $\otimes$  denotes convolution.

This model for the imaging process in optical systems can be applied to the eye and is widely accepted. It has been illustrated in numerous texts via simulation, in which an image is blurred by convolution with a broad PSF, representing a level of defocus, (Figure 2) [15, 16]. Under these same assumptions, the degraded retinal image can be reconstructed through an inverse process, given by

$$U(x, y) = U'(x, y) \otimes H^{-1}(x, y) \quad (2)$$

where  $H^{-1}(x,y)$  is the inverse of the PSF.

This inverse process is referred to as "deconvolution". The process of deconvolution is the convolution of the blurred image with the inverse of the PSF. The deconvolution recovers the undistorted image. If instead, the deconvolution is applied to the undistorted image, a pre-compensated image will be created. When viewed through the PSF, this pre-compensated image will be projected onto the retina, free of distortion. This process is illustrated by

$$U(x, y) = (U(x, y) \otimes H^{-1}(x, y)) \otimes H(x, y) \quad (3)$$

In order to use computers efficiently, in addition to reading text, a user must be able to navigate in the GUI through the use of icons [11, 12]. Figure 3 illustrates an example of what a user with a severe low-order aberration would face when interfacing with a computer via icons. The PSF used for this simulation is shown in Figure 4. Figure 3-b exemplifies the difficulty a user would face when trying to identify various icons to perform ordinary tasks.

Deconvolution does not have a precise mathematical definition and is reputed as mathematically ill-posed because it may yield multiple solutions. However, the practical importance of the deconvolution concept has prompted the design of several methods for its implementation [1, 4].

## 3. APPROACH

Recently developed "Wavefront Analyzers" based on the Hartmann-Shack Principle have made it possible to measure the wavefront aberration function for the human eye. These wavefront analyzers are becoming common in many ophthalmologists' offices.

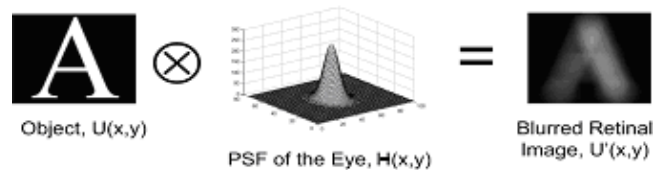


**Figure 2. Block diagram of human eye as an LTI**

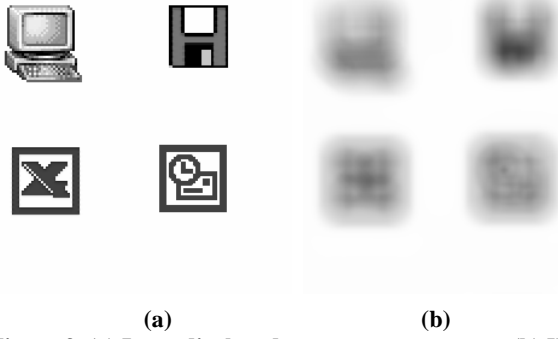


**Figure 3. (a) Icons displayed on a computer screen (b) What the user with a severe spherical aberration would perceive**

The wavefront aberration function,  $W(x,y)$ , is the primary component of the pupil function,  $P(x,y)$ , which incorporates the complete information about the imaging properties of the optical system [18]. The pupil function is given by the following:

$$P(x, y) = A(x, y)e^{-j2\pi nW(x,y)/\lambda} \quad (4)$$

where  $A(x,y)$  is the amplitude function describing the relative efficiency of light passing through the pupil (usually given a value of one),  $n$  is the index of refraction, and  $\lambda$  is the wavelength of light in a vacuum [15].

According to the Fourier optics relationships in the eye, knowledge of the pupil function can be used to determine the optical transfer function, OTF, which is “one of the most powerful descriptors of imaging performance for an optical system” [18]. The OTF is a complex function whose magnitude is the modulation transfer function (MTF) and whose phase is the phase transfer function (PTF) [15].

The OTF can be found by convolving the pupil function,  $P(x,y)$ , with its complex conjugate,  $P^*(-x,-y)$  [6, 15, 16, 19]:

$$O(fx, fy) = P(x, y) \otimes P^*(-x, -y) \quad (5)$$

This is equivalent of saying that the OTF is the autocorrelation of the pupil function. The PSF and the OTF are a Fourier transform pair [19]:

$$O(fx, fy) = F\{H(x, y)\} \quad (6)$$

Once the PSF is obtained for the user’s eye, it is used in the deconvolution process.

Wavefront technology is “an exciting, new field currently being developed in the ophthalmic community” [9]. As such, wavefront analysis technology is becoming a common element in the set of tools that many ophthalmologists or optometrists use for diagnosing the refractive errors of the eye [20]. Thus, it is not unreasonable to expect that in the near future, patients will have access to their wavefront aberration information. This will allow for a customized pre-compensation scheme in their computers.

### 3.1 Deconvolution Overview

Inverse filtering is traditionally used in image processing to restore an image  $U(x,y)$  from a degraded image  $G(x,y)$ , assuming a known degradation function,  $H(x,y)$  [5]. As stated above, the

input and output of any linear system are related through the convolution operator. That is,

$$G(x, y) = U(x, y) \otimes H(x, y) \quad (7)$$

If the Fourier principles of convolution are applied,  $U(x,y)$  can be obtained as follows:

$$U(x, y) = F^{-1}\left\{\frac{F\{G(x, y)\}}{F\{H(x, y)\}}\right\} \quad (8)$$

where  $F\{\}$  and  $F^{-1}\{\}$  denote the Fourier transform and the inverse Fourier transform, respectively.

In the context of pre-compensation of a digital image to be shown to the viewer, the objective is to deconvolve the PSF of the viewer’s eye,  $H(x, y)$ , from the intended digital image,  $I(x, y)$ , in order to derive the pre-compensated display image to show on-screen,  $RD(x, y)$ . This calculation of  $RD(x, y)$  is practically accomplished as:

$$RD(x, y) = F^{-1}\left\{\frac{F\{I(x, y)\}}{F\{H(x, y)\}}\right\} \quad (9)$$

The denominator within the braces of equation 9 is the OTF of the viewer’s eye.

This implementation of inverse filtering has several limitations, however, especially for values of the OTF which are close to zero. A common approach to circumvent this problem is the use of Minimum Mean Square Error (Weiner) filtering [5]. In the context of the problem at hand, this approach obtains the pre-compensated image as:

$$RD(fx, fy) = \left[ \frac{1}{H(fx, fy) \left[ |H(fx, fy)|^2 + K \right]} \right] I(fx, fy) \quad (10)$$

where  $RD(fx,fy)$ ,  $H(fx,fy)$ , and  $I(fx,fy)$  are the Fourier transforms of  $RD(x,y)$ ,  $H(x,y)$ , and  $I(x,y)$ , respectively.

For the example in Figure 3, the user’s PSF is shown in Figure 4. Following the method outlined above and applying it to Figure 3-a, using the PSF in Figure 4, a pre-deconvolved image is generated (Figure 5-a). This image is then viewed through the visual aberration.

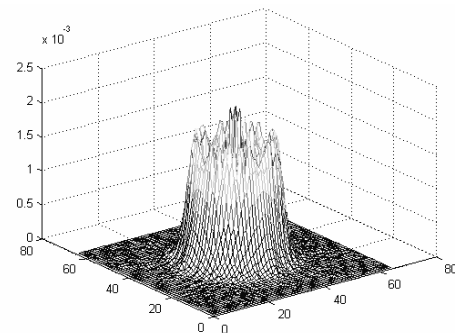


**Figure 4. Broad PSF due to visual impairment**

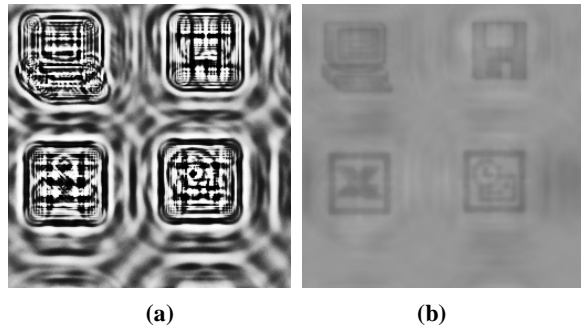


**Figure 5. (a) Result of pre-compensation (what is displayed to the user) (b) What the user with the aberration shown in Figure 4 would perceive when viewing (a)**

The result (Figure 5-b) shows that the pre-compensation has reverted some of the acuity loss introduced by the aberration. This enhancement of the effective visual acuity is likely to facilitate a user's interaction with the computer, as previous research has demonstrated that visual acuity is an important factor in the usability of GUI's by users with low vision [11].

It should be noted that Figures 3-b and 5-b are software simulations using the methods outlined above. In order to demonstrate the method in a more realistic context, Figures 6 – 9 display pictures taken through a digital camera simulating the visual system of a user interacting with the GUI. A fixed and known defocus was introduced in the field of view of the camera to simulate a visual aberration. Figure 9 confirms the ability of this method to preserve the acuity of the image. However, this figure also shows a loss of contrast due to the intensity scaling that must be applied to the pre-compensated image in order to display it on the computer monitor. Thus, performance of this approach is ultimately influenced by the ability of the computer monitor to accurately reproduce the required intensities. Current work focuses on suitable post-processing of the pre-compensated image to minimize this effect.

#### 4. EVALUATION

In order to assess the effectiveness of the pre-compensation with a known and fixed wavefront aberration, a -6 diopter spherical lens was interposed in the field of view of a digital camera (Sony Mavica MVC-FD95). This camera shows the image to the user in a 2.5" LCD display with 800 x 225 pixel resolution.

Since the ability to efficiently use an interface does not depend solely on the perception abilities of the user, but also involves higher-level cognitive processes to integrate and react to the perceptual input received, it was important to evaluate the potential gains of using pre-compensated images in a context that involved pattern recognition by human users. Accordingly, the evaluation of the system was performed by emulating a common visual acuity assessment, asking test subjects to recognize the letters on a Bailey-Lovie logMAR (logarithm of the minimum angle of resolution) eye test chart, with "Sloan" letters [3]. This type of chart and its associated visual acuity measure (logMAR) were preferred over the Snellen visual acuity test chart because of several advantageous characteristics that would benefit this evaluation process [2], namely:

- The letter size progression is in uniform steps on a logarithmic scale so that the scaling factor is constant throughout the chart and will remain unaltered when non-standard viewing distances are used
- Each row of the chart has the same number of letters (5)
- The letters present in all the lines are equally legible.
- Consistent spacing between letters (1 letter width)
- Consistent spacing between rows (the space is equal to the height of letters in the smaller row).

In addition, Holladay [10] has proposed that the logMAR units are the appropriate units to involve in statistical calculations of visual acuity. Figure 10 shows an example of a Bailey-Lovie logMAR chart.

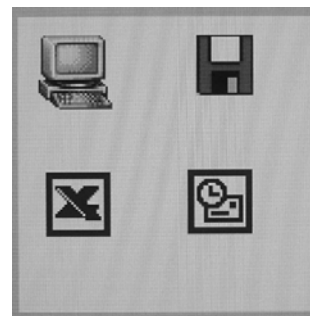


**Figure 6. Intended image captured by the camera, without blur**

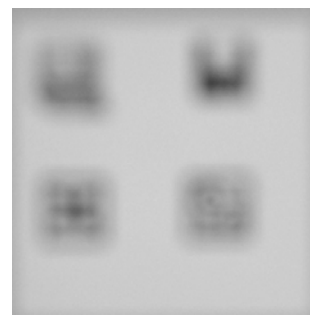


**Figure 7. Intended image captured by the camera, with blur**

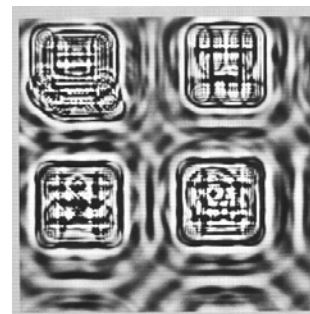


**Figure 8. Pre-compensated image captured by the camera, without blur**

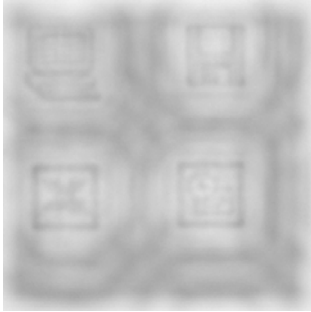


Figure 9. Pre-compensated image captured by the camera, with blur

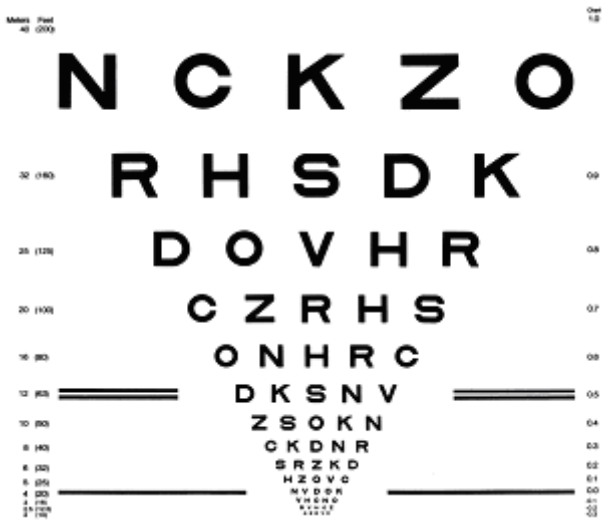


Figure 10. An example of a Bailey-Lovie logMAR eye test chart using 'Sloan' letters

#### 4.1 Evaluation levels

The use of the digital camera with the fixed  $-6$  diopter lens ensured that the wavefront aberration for all the experimental subjects would be the same. This allows for the same set of pre-compensated images to be used for all the subjects. On the other hand, this also introduced an inherent acuity limit. At the chosen test distance of 2 meters, the bars making up the letters of a given line in the chart have a specific width. When viewed through the limited resolution of the LCD display panel in the digital camera, the segments of the smallest letters (lines 13 and 14, with nominal logMAR values of  $-0.2$  and  $-0.3$  for the default viewing distance of 4 meters) will not be resolved in the display. This instrumental limitation made it necessary to also ask the subjects to read the letters in the chart without the blurring lens interposed in the field of view, defining the “baseline acuity” for subjects with corrected vision in this instrumental setup.

Therefore, participating subjects viewed the simulated eye chart displayed on a computer monitor under three different conditions:

- a) *Standard*: The (focused) digital camera was used to view the computer monitor without any interposed blurring lens. Normal images, emulating individual lines of the Bailey-Lovie chart were displayed.

- b) *Blurred*: The  $-6$  diopter blurring lens was placed in front of the camera. Normal images, emulating individual lines of the Bailey-Lovie chart were displayed.
- c) *Pre-compensated*: The  $-6$  diopter blurring lens was placed in front of the camera. In this case, the images shown in the computer monitor were pre-compensated versions of the original Bailey-Lovie rows, obtained using the PSF estimated for the  $-6$  diopter spherical lens.

#### 4.2 Hypothesis

The hypothesis explored through this experimentation was:

The display of pre-compensated digital images, as opposed to normal or “direct” images, will result in a significantly better effective visual acuity.

#### 4.3 Subjects

Fourteen college student volunteers (9 male and 5 female) participated in the evaluation of the system. Approval from the Institutional Review Board at Florida International University was obtained for this experiment involving human subjects. Each individual participant was briefed on the steps involved in the experiment and provided informed consent to the participation.

Since logMAR acuity is commonly evaluated on a monocular basis for clinical purposes, the evaluation performed for this research was also monocular. A total of 28 eyes were involved in the tests, and each was identified by a numerical “Eye ID”. All of the participants were asked to use their spectacles or contact lenses and were considered to have fully corrected vision. Therefore, the pre-compensated images were developed on the assumption that the  $-6$  diopter lens would introduce the totality of the wavefront aberration that need to be compensated. None of the subjects reported uncorrected visual limitations.

#### 4.4 Procedure

Each subject was asked to view and read the simulated rows of the Bailey-Lovie chart from the computer monitor, by looking at the LCD panel in the back of the digital camera. The participant would continue reading complete rows down the chart until errors were made, under each one of the three conditions identified above: Standard, Blurred and Pre-compensated, first with one eye and then with the other. The order of this eye sequence was randomized.

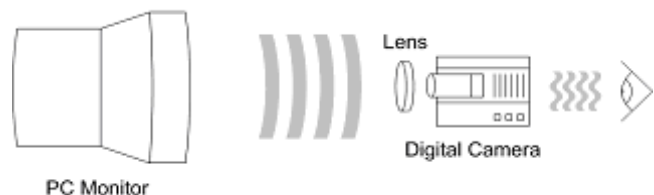


Figure 11. General instrumental setup for the evaluation process

The sequence of the conditions implemented for each subject was also randomized. Figure 11 shows the instrumental configuration used (the lens was not used for the “Standard” experimental condition).

## 5. RESULTS

### 5.1 Measurements

For each reading of the Bailey-Lovie chart the letters correctly read and those incorrectly read were recorded and the corresponding logMAR score (corrected for the chosen testing distance of 2 meters) was calculated. To determine the true logMAR value,  $X$ , in a case in which the subject correctly read the complete row corresponding to a logMAR value  $cLV$ , and only  $n < 5$  letters from the next line, the following formula can be used [10]:

$$X = cLV - 0.1(n/5) \quad (11)$$

Once the logMAR value  $X$  is determined, the “decimal acuity”,  $V$ , can be found as [10]:

$$V = 10^{-X} \quad (12)$$

and the, so-called “Visual Efficiency”,  $E$ , defined by the American Medical Association, can be found through the following equations [3]

$$\log E = -0.0777A + 2.0777 \quad (13)$$

and

$$A = \frac{2.0777 - \log E}{0.0777}, \quad (14)$$

where

$$A = 1/V. \quad (15)$$

Table 1 displays the mean and standard deviation of the logMAR values recorded from the 28 eyes studied, under each of the 3 experimental conditions. This table also includes the average visual efficiency value, and associated standard deviation, for each condition.

From the table, it should be noted that, although the pre-compensation did not fully return the performance of the subjects to the levels achieved in the unimpaired, “Standard” condition (mean logMAR = 0.33,  $E = 81.39\%$ ), it indeed improved with respect to the severely restricted acuity recorded for the impaired, uncompensated condition (“Blurred”), which recorded a mean logMAR value of 1.37 and a mean visual efficiency of only  $E = 1.92\%$ .

With the display of pre-compensated images viewed through the blurring lens the mean logMAR acuity and the mean visual efficiency reached values of 0.67 and 51.69%, respectively. The similarity of the behavior across the 28 eyes studied, with respect to the three experimental conditions tested is shown in Figure 12, which displays the logMAR acuity values for all eyes under the three conditions.

**Table 1: Summary of the Experimental Results**

Experimental Condition	Mean LogMAR Acuity	Std. Dev. LogMAR Acuity	Mean Visual Efficiency	Std. Dev. Visual Efficiency
Standard	0.33	0.05	81.39 %	3.38 %
Blurred	1.37	0.05	1.92 %	1.36 %
Pre-compensated	0.67	0.04	51.69 %	4.22 %

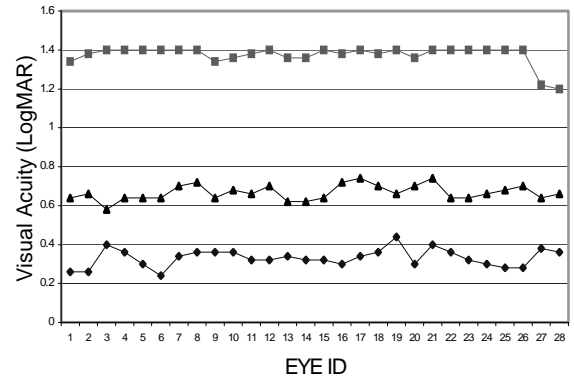


**Figure 12. LogMAR acuity measurements under the three conditions tested: “Standard” (Diamonds), “Blurred” (Squares), and “Pre-compensated” (Triangles)**

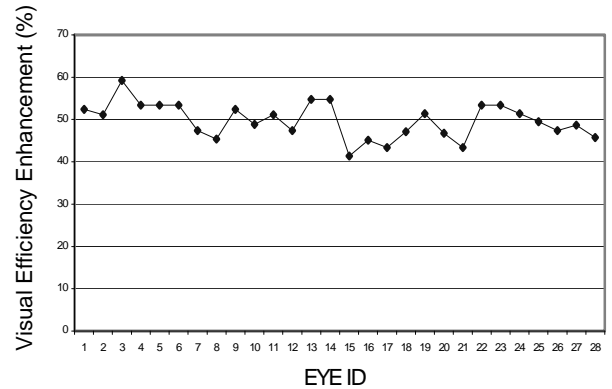


**Figure 13. Visual efficiency enhancement,  $\Delta E = E_{precomp} - E_{blurred}$ , achieved by displaying pre-compensated images**

In order to address the main question behind the experiment, the difference in visual efficiency for the two impaired viewing conditions established by the display of pre-compensated images or original (direct) images, i.e.,  $\Delta E = E_{precomp} - E_{blurred}$ , was calculated for each one of the 28 eyes. Figure 13 displays these values.

### 5.2 Data Analysis

A dependent t-test was performed using the Statistical Package for the Social Sciences (SPSS), V.9. The results confirmed that there was a significant difference ( $t(27)=64.89$ ,  $p<0.01$ ) in the logMAR acuity recorded when the direct images were displayed

("blurred" condition) and when the pre-compensated images were displayed ("Pre-compensated" condition). The display of pre-compensated images considerably reduced the mean logMAR acuity from 1.37 to 0.67, and limited the standard deviation of the logMAR measurements (from 0.05 to 0.04).

## 6. CONCLUSION

The simulations and imaging tests performed with a digital camera have illustrated the potential of the image pre-compensation approach proposed to revert the degradation on the perception of visual interface elements. Furthermore, the evaluation conducted with human subjects resulted in improved visual acuity scores recorded when the pre-compensated images were used. The statistical analysis performed on the experimental data supports the hypothesis that displaying the pre-compensated images provides a significant enhancement of the effective visual acuity of the user.

The next stage of our work will use the methods developed to generate the pre-compensation for participants with targeted visual impairments, preferably of high-order. This will allow verification of the general applicability of the algorithms.

We envision that this pre-compensation approach will be applicable to users with severe refractive errors whose individual wavefront aberration functions can be obtained using wavefront analyzers, as these instruments are becoming a common tool used by many ophthalmologists and optometrists.

## 7. ACKNOWLEDGMENTS

This work was sponsored by NSF grants IIS-0308155 and HRD-0317692. Mr. Miguel Alonso Jr. is the recipient of an NSF Graduate Research Fellowship.

## 8. REFERENCES

[1] Alonso, J., M. and A.B. Barreto, *An Improved Method of Pre-Deblurring Digital Images Towards the Pre-Compensation of Refractive Errors*. WSEAS Transactions on Computers, 2004. 3(2): p. 487-492.

[2] Bailey, I.L. and J.E. Lovie, *New design principles for visual acuity charts*. American Journal of Optometry, 1976. 57: p. 378-387.

[3] Bennet, A.G. and R.B. Rabbetts, *Clinical Visual Optics*. 1989, London: Butterworths.

[4] Gonsalves, R.A. and P. Nisenson, *HST Image Processing: An Overview of Algorithms for Image Restoration*. SPIE Applications of Digital Image Processing, 1991. 1567(14): p. 294-307.

[5] Gonzales, R.C. and R.E. Wood, *Digital Image Processing*. 2002, New Jersey: Prentice Hall.

[6] Goodman, J.W., *Introduction to Fourier Optics*. McGraw-Hill Physical and Quantum Electronics Series. 1968, New York: McGraw-Hill Book Company.

[7] Guyton, A.C. and J.E. Hall, *Textbook of Medical Physiology*. 1996, Philadelphia: Saunders Company.

[8] Higuchi, K., T. Nakano, and S. Yamamoto, *Simulating Human Vision Based on Adaptation and Age-related Visual Changes*. R and D Review of Toyota CRDL, 2000. 35(2).

[9] Hjortdal, J., *Book Review: Wavefront and Emerging Refractive Technology*. ACTA Ophthalmologica Scandinavia, 2003. 81(6): p. 681.

[10] Holladay, J.T., *Proper method for Calculating Average Visual Acuity*. Journal of Refractive Surgery, 1997. 13: p. 388-391.

[11] Jacko, J.A., et al. *Low Vision: The Role of Visual Acuity in the Efficiency of Cursor Movement*. in *Fourth International ACM Conference on Assistive Technologies (ASSETS '00)*. 2000. Arlington, VA: ACM.

[12] Kline, R.L. and E.P. Glinert. *Improving GUI Accessibility for People with Low Vision*. in *CHI'95 Conference on Human Factors in Computing Systems*. 1995. New York: ACM.

[13] Liang, J., Williams, D.R. , and Miller D.T., *Supernormal vision and high-resolution retinal imaging through adaptive optics*. Journal of the Optical Society of America, 1997. 14: p. 2884-2892.

[14] Parker, J.N. and P.M. Parker, *The official patient's sourcebook on Keratoconus: A revised and updated directory for the internet age*. 2002, San Diego: Icon Health Publications.

[15] Salmon, T.O., *Corneal Contribution to the Wavefront Aberration of the Eye*, in *School of Optometry*. 1999, Indiana University.

[16] Thibos, L.N., *Formation and Sampling of the Retinal Image*, in *Seeing*, K.K.D. Valois, Editor. 2000, Academic Press: California.

[17] Thibos, L.N., X. Qi, and D.T. Miller, *Vision through a liquid crystal spatial light modulator*, in *Adaptive Optics for Industry and Medicine*, G. Love, Editor. 1999, World Scientific Press.

[18] Williams, C.S. and O.A. Becklund, *Introduction to the optical transfer function*. Wiley series in pure and applied optics. 1989, New York: Wiley. xi, 412.

[19] Wilson, R.G., *Fourier Series and Optical Transform Techniques in Contemporary Optics: An Introduction*. 1995, New York: John Wiley and Sons, Inc.

[20] Young, M., *AAO preview: A close look at wavefront*. EyeWorld, September, 2003: p. 30.